Chapter 6

Evaluation of Harmonic Risk in Offshore Wind Farms

The interaction between the offshore installations and the onshore grid can cause harmonic amplifications. This aspect is not trivial, because as a result of this harmonic amplification, the harmonic level in the point of common coupling of the wind farm can be unacceptable for the grid code requirements.

Offshore wind farms are connected through a widespread medium voltage submarine cable network and connected to the transmission system by long high voltage cables. Submarine power cables, unlike underground land cables need to be heavily armored chapter 4 and are consequently complicated structures. So, in particular this type of power cables have a relatively larger shunt capacitance compared to overhead lines which make them able to participate more in resonant scenarios [25].

The present chapter evaluates the frequency behavior of the offshore wind farms at normal operation (steady state), depending on the design procedure parameters like: the cable length / characteristics, transformers connection and leakage inductance or inter-turbine grids configuration. The analysis is performed from the point of view of the wind turbines, considering them as potential harmonic sources. Thus, the knowledge of the frequency behavior of the offshore wind farm can help to avoid as much a possible the harmonic amplification, at the design stage of the wind farm. This presents new challenges in relation to understanding the nature, propagation and effects of the harmonics.

6.1 Harmonics in distribution grids

Nowadays, the state of the distribution grids is significantly different in comparison with the state of two decades ago. The main reason is the existence of no lineal loads. These no lineal loads provoke disturbances, like a high level harmonics in current and voltages [104].

In the same way, there is consolidating a distributed generation system for the distribution grids. This kind of grids have a combination of many types of generation plants, such as cogeneration, combined cycle, wind farms, photovoltaic…Thus, if the distribution grid is made up with many little and medium generation plants, the waveform of the voltage may be distorted.

In conclusion, the electric transmission system is evolving to a scenario with multiple harmonic sources. So, the frequency analysis of the electric grids is becoming an important tool, because can help to improve their efficiency reducing the power associated to these disturbances.

The current and voltage harmonics superimposed to the fundamental wave causes several negative effects in the devices connected to the distribution grid.

The harmonic currents are the cause of the distortion of the voltage wave in different points of the distribution system, i.e. the circulation through the electric grids of these currents provokes distorted voltage drops, so, at the system nodes there are not pure sine waves. Thus, the bigger are the harmonic currents of the power system, more distorted are the voltages in the nodes and bigger the negative effects caused by them.

Therefore, the system operators of the energy distribution grids have specific rules to limit the harmonic emission, for both of them, voltage and current.

6.2 Main disturbances caused by current and voltage harmonics

The distorted voltages are the cause of many negative effects to the devices connected to the system. These effects are: The reduction of the devices lifetime, the degradation of the efficiency and the degradation of the operation in general.

The negative effects caused by the harmonics depends on the type of the load and these negative effects can be divided into two groups [105]:

- Instantaneous effects.
- Long-term effects due to the heating.

Instantaneous effects:

- Displacement of the zero crossing of the voltage wave and because of this the switching conditions of the thyristors.
- Additional errors in induction disks of the electric meters.
- Vibrations and noise, especially in electromagnetic devices (transformers, reactors, etc…).
- Pulsating mechanical torques, due to changes in the value of the instantaneous current.
- Malfunction of the protection devices, like fuses, breakers and digital equipment's for protection [106]. In the case of a system protected against the overvoltage, where the protections are designed to operate with sinusoidal voltages, cannot operate correctly with non-sinusoidal waveforms. The operation can go wrong, from the overprotection of the system to the non-protection of it.

Long-term effects: The main long-term effect of the harmonics is the heating of the devices.

Heating of the capacitors: The losses caused by the harmonics are transformed into heat. In the specific case of the capacitor, these losses are: conduction losses and hysteresis losses in the dielectric.

Heating due to additional losses in machines: There are additional losses at the stator (cupper and iron) and at the rotor (magnetic circuit and the coil). These losses are caused by the speed difference in the inductive rotating field between the rotor and stator.

Heating of the transformers: Additional losses due to the skin effect, there is a increment of the resistance for harmonic currents. In the same way, there are also additional losses in the magnetic circuit (Foucault currents) and hysteresis.

Heating of the cables: In cables where are circulating harmonic currents, there are additional losses due to:

- An increment in the apparent resistance due to the skin effect.
- An increment in the effective current for the same active power.
- An increment in the dielectric losses in the insulation with the frequency, if the applied voltage to the cable is significantly distorted.

In Table 6.1, extracted from [107], the negative effects caused by harmonics to electric devices are summarized.

Effects of the harmonics	***Cause***	***Consequence***
Upon the conductors	• *An increment of the Irms.* • *The skin effect, which reduces the effective area of the conductor.*	• *Malfunction of the protections.* • *Overheating of the conductors.*
Upon the transformers	• *An increment of the Irms.* • *Increments in the Foucault losses due to there are proportional to the square of the frequency.*	• *An increment of the heating of the coils due to the Joule effect.* • *An increment of the losses in the iron.*
Upon the capacitors	• *A decrement of the capacitors impedance with the frequency.*	• *Premature aging and the amplification of the harmonics.*

Table 6.1 Negative effects caused by harmonics to electric devices.

In order to prevent these disturbances, the elimination of all the harmonic components to obtain a pure sine wave is impossible. However, it is possible to achieve a good approximation to a sine wave. For that purpose, there are operation standards and grid codes.

One of those is the IEEE-519 standard, in this standard there are set up the limits of the harmonic amplitudes for current and voltage. For the specific case of the main distribution grid, the harmonic limits are shown in Table 6.2 and Table 6.3.

IEEE-519 Harmonic current limits for HV systems.

IEEE-Maximum odd harmonic currents for main distribution system, for 69,001kV to 161kV.

I_{SC}/I_L	n < 11	11 ≤ n ≤ 17	17 ≤ n ≤ 23	23 ≤ n ≤ 35	35 ≤ n	*THD*
<20	2.0 %	1.0 %	0.75 %	0.3 %	0.15 %	2.5 %
20-50	3.5 %	1.75 %	1.25 %	0.5 %	0.25 %	4.0 %
50-100	5.0 %	2.25 %	2.0 %	0.75 %	0.35 %	6.0 %
100-1000	6.0 %	2.75 %	2.5 %	1.0 %	0.5 %	7.5 %
>1000	7.5 %	3.5 %	3.0 %	1.25 %	0.7 %	10.0 %

Table 6.2 Harmonic current limits for high voltage systems.

IEEE-519 Voltage limits.

IEEE-Voltage distortion limits.

BUS voltage at the PCC	*Individual harmonics*	*THD*
69kV and smaller	*3.0 %*	*5.0 %*
69,001kV to 161kV	*1.5 %*	*2.5 %*
Over 161kV	*1.0 %*	*1.5 %*

Table 6.3 Harmonic voltage limits for high voltage systems.

6.3 Frequency response of the transmission system via PSCAD simulation

6.3.1 Frequency response of the submarine cable

The frequency response of the submarine cable described in this chapter is based on the model of the submarine cable analyzed and validated in chapter 4. Thus, the present analysis considers this model as a reasonably accurate approximation.

One option to carry out the frequency response analysis in an easy way is the use of the impedance meter provided by PSCAD in its standard library, but this impedance meter have not taken into account completely the validated model.

As is highlighted in the PSCAD user's manual [64], this impedance meter cannot correct the curve fitting errors during the simulation. Thus, in the present analysis, the simulation scenario depicted on Figure 6.1 is used. The simulation of this scenario takes into account the complete cable model and in consequence the results are intended to be more accurate.

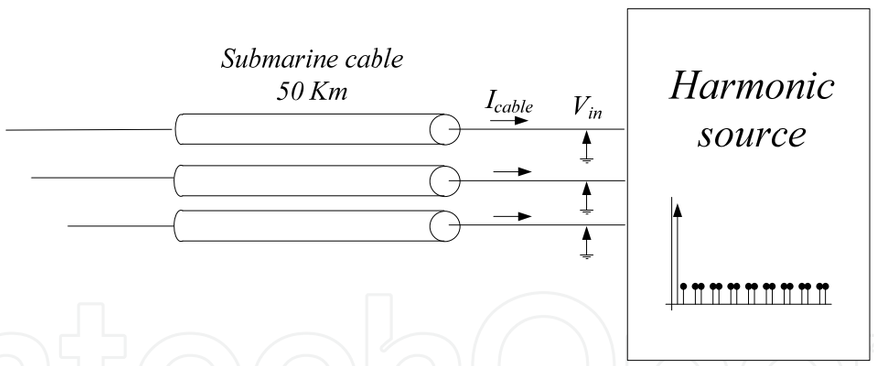

Figure 6.1 Simulation scenario to obtain the frequency response of the submarine cable.

As regards to this scenario, to calculate the impedance of the submarine cable depending on the frequency, a harmonic voltage source is used. So, the harmonic voltage source applies a harmonic train to the submarine cable, which is connected as a load. The cable is the same of the used in chapter 4, its characteristics are shown in Table 4.2.

The harmonic train of input voltage (V_{in}), is composed by sinusoidal components in the range of frequencies: 50-5000Hz. The amplitude of these harmonic voltages is 10% of the fundamental (50Hz-150kV). Starting from the 50Hz, the harmonic train has voltage components separated 10Hz one from other, as illustrated in Figure 6.2. These input harmonics in a simplified way can represent the effect of the harmonics generated by the wind turbines, when they are generating energy from the wind.

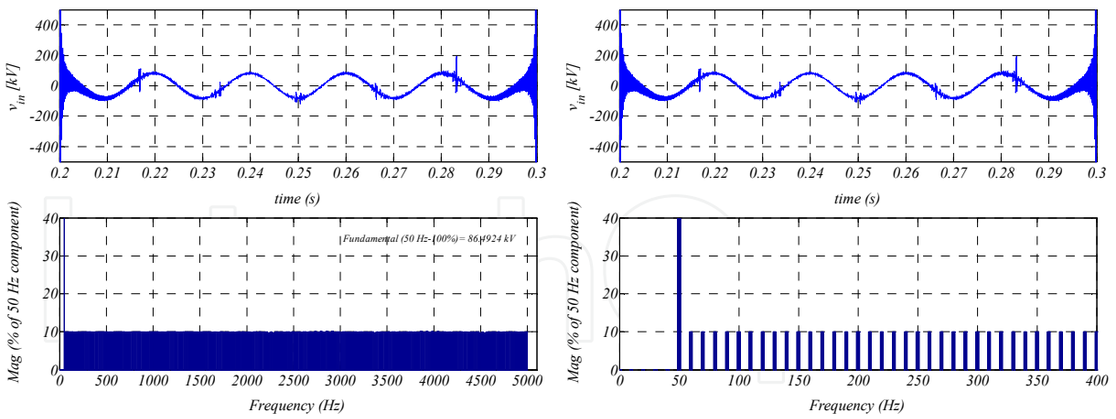

Figure 6.2 Harmonic voltage train applied to the submarine cable model. Resolution 10 Hz.

Measuring the current at the PCC (I_{pcc}) and performing the FFT (Fast Fourier Transform) of the signal, Figure 6.3, it is possible to obtain the impedance of the transmission system for each one of the excited frequencies, i.e. it is possible to obtain the evolution of the impedance depending on the frequency.

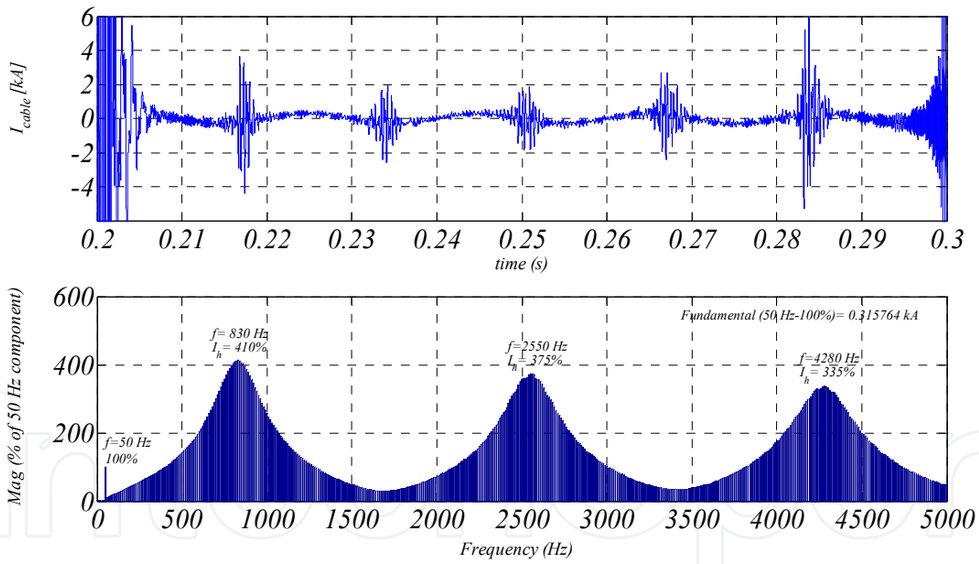

Figure 6.3 Frequency response of the submarine cable via PSCAD simulation for a 50 Km cable, resolution 10 Hz.

Looking at the results depicted in Figure 6.3, the specified cable has several frequencies where the harmonics are amplified. In the analyzed range (50-5000Hz), there are three harmonic groups: around 830Hz, around 2550 Hz and around 4280Hz.

6.3.2 Frequency response of the transmission system via PSCAD simulation

The transmission system is the part of the offshore wind farm which makes possible the energy transmission from the collector point (offshore) to the point of common coupling

(onshore), in other words, the physic medium to transfer the energy from the wind farm to the main grid and all the support devices.

The transmission system is made up by the step-up transformer, the submarine cable, reactive power compensation elements (if required), and the support devices to integrate the energy in the main grid (if required).

The knowledge of the frequency response of the transmission system and the influence of each component upon this frequency response can help to avoid undesired resonances and harmonics. For that purpose, firstly, in this section the simplest lay-out for the transmission system (transformer, cable and grid, Figure 6.4) is considered, i.e. the necessary elements to perform the energy transmission, without the support devices to improve the transmission.

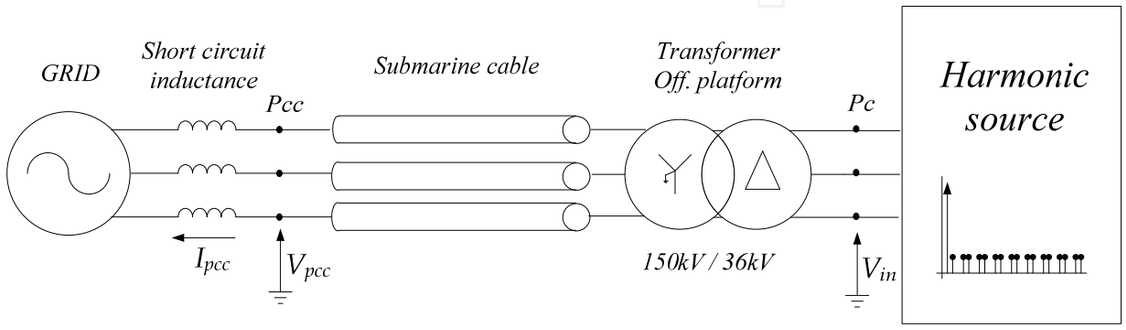

Figure 6.4 Simulation scenario of the simplest lay-out of the transmission system: the step-up transformer, the submarine cables and the distribution grid.

In this case also is performed the same procedure to obtain the frequency response used in the previous section (6.3.1).

To model the grid in a simple manner, a voltage source and short circuit impedance is used. Its characteristics are summarized in Table 6.4. The transformer's connection is Δ- gY, while its characteristics are shown in Table 6.5. Finally, the cable characteristics and cable model are the same of the section 6.3.1

Parameter	Value
Nominal power (Pn)	150 MW
Nominal voltage (Vn)	150 kV
Short circuit inductance	5 %

Table 6.4 Characteristics of the main grid.

Parameter	Value
Rated power	150 MVA
Primary voltage	33 kV
Secondary voltage	150 kV
Connection	Δ- gY
Transformers leakage resistance	1 %
Transformers leakage inductance	6 %
No load losses	1,78 %

Table 6.5 Characteristics of the step-up transformer.

The frequency response of the described transmission system layout is depicted in Figure 6.5.

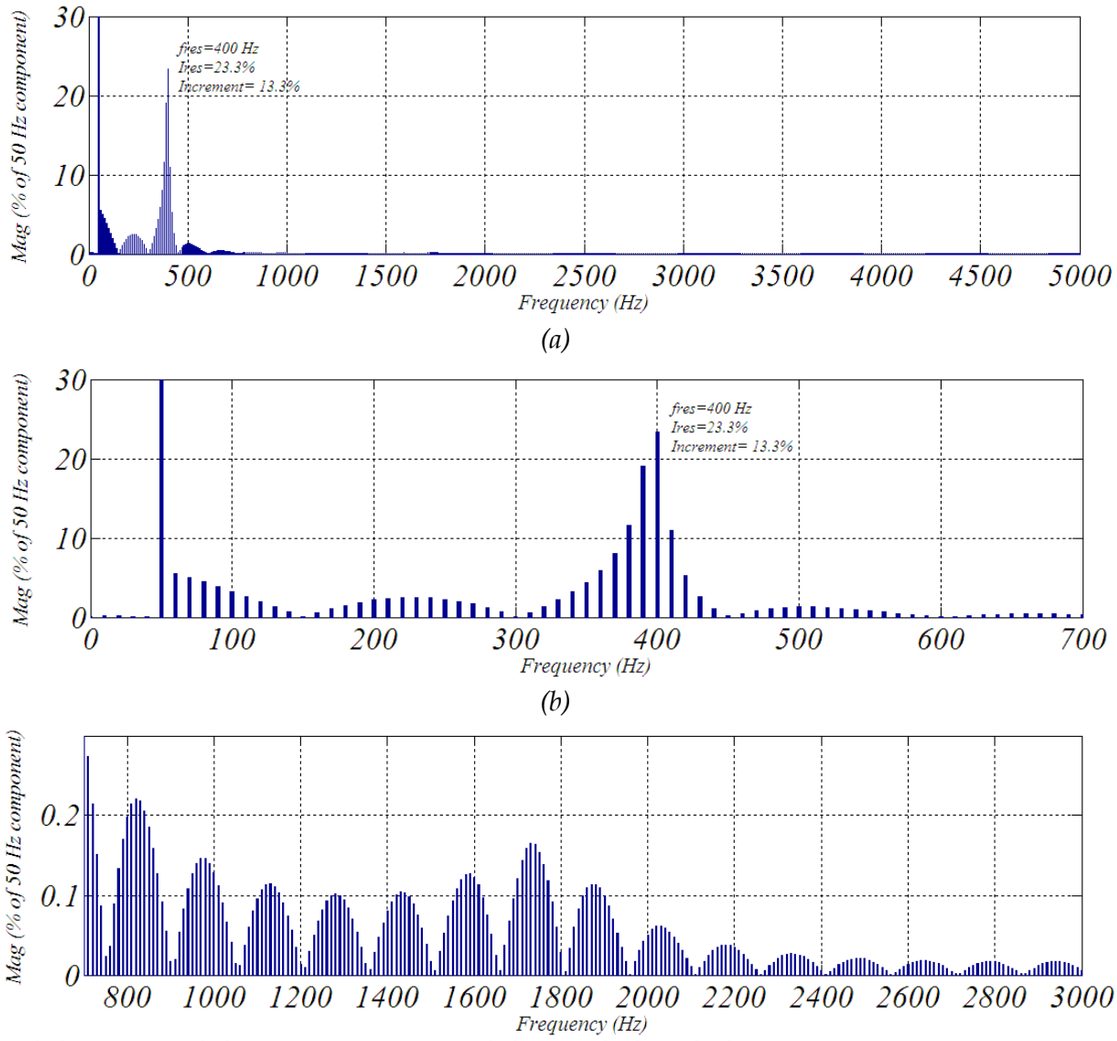

Figure 6.5 Frequency response of the transmission system with only: step-up transformer and submarine cables. FFT of the current at PCC. (a) Whole analyzed spectrum, (b) more detail in the main resonance and (c) more detail in high frequencies.

Looking at Figure 6.5, it is possible to observe that all the multiples of the 3rd order harmonics generated in the wind turbines, cannot trespass to the PCC. This occurs because between these points is placed a transformer with star (grounded)-delta connection.

The transmission system is composed with several inductive components, like the transformer or the short circuit impedance of the main grid. This inductive impedances provokes a significant attenuation of the high frequencies, as can be seen in Figure 6.5 *(c)*, thus, the high frequency harmonic voltages do not affect to the current of the PCC. In fact, in

the present analysis, the harmonics higher than 700Hz almost do not affect to the current at PCC.

However, the interaction of the inductive component of the transmission system with the capacitive component of the submarine cable provokes a resonance at 400Hz, becoming these frequencies which are around the 400Hz potentially problematic.

6.3.3 The effect of the main components in the frequency response of the transmission system

The analysis of how affects each one of the elements of the transmission system in its frequency response is the first step to avoid undesired resonances and optimize the transmission system design.

Therefore, this section analyses the frequency response of the transmission system varying the characteristics (impedance) of its three main components:

- The leakage impedance of the step-up transformer.
- The impedance of the submarine transmission line (variation of the cable length).
- The short circuit impedance of the main grid.

Firstly, the influence of the step-up transformer is evaluated. Based on the scenario illustrated in Figure 6.4 and applying the same harmonic train (Figure 6.2), the frequency responses of the transmission system are obtained. In this first case, the transformer's leakage inductance has a variation from 3% to 12%, the results are depicted in Figure 6.6.

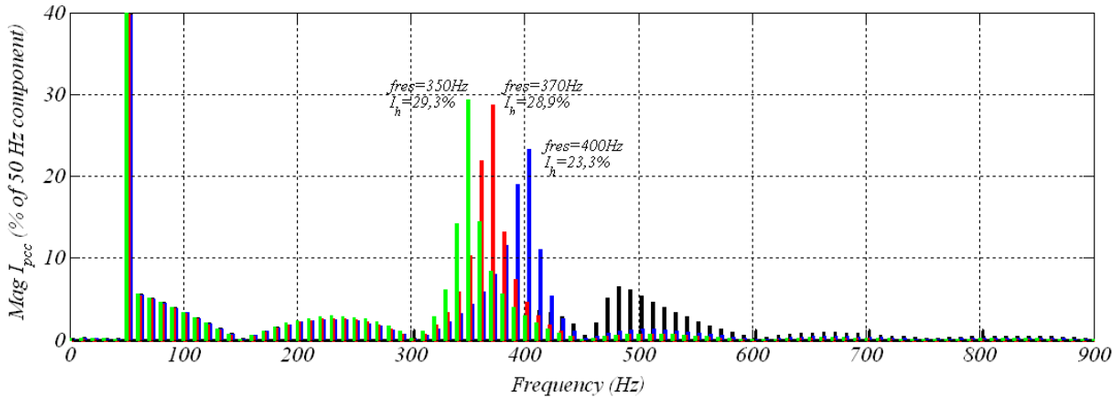

Figure 6.6 Frequency response of the transmission system varying the leakage inductance of the step-up transformer from: 3% (black), 6% (blue), 9% (red) and 12% (green).

As is shown in Figure 6.6, as the leakage inductance of the step-up transformer increases, the frequency of the resonance decreases (from 450Hz to 350Hz).

For the specific case where the leakage inductance is 3%, it is possible to see how the transformer connection does not allows to cross to the PCC the harmonics close to the resonance, Figure 6.7. The resonance is still there (450Hz), but, there are not harmonics to be amplified.

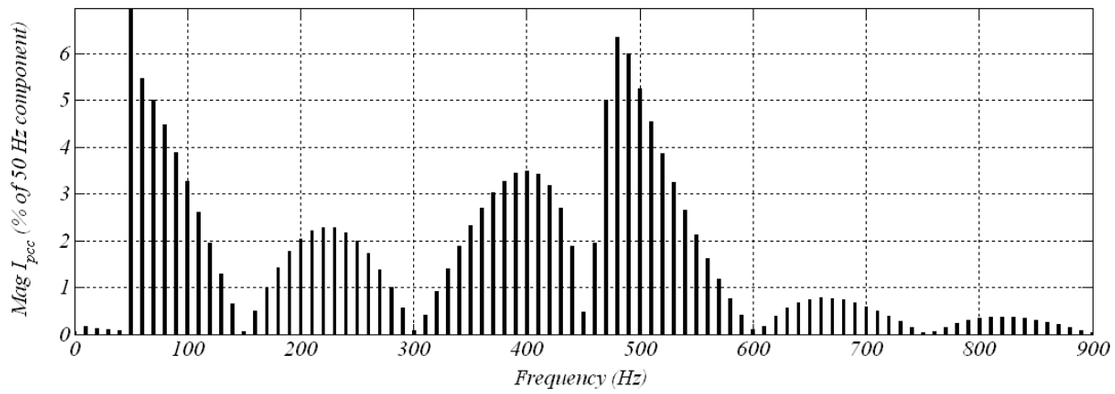

Figure 6.7 Frequency response of the transmission system with a leakage inductance of 3% of the step-up transformer.

The harmonic train used for this analysis has components into de 50-5000Hz range, but not continuously in all this range, the harmonic source generates harmonic voltages in steps of 10 Hz. Thus, using the harmonic train is possible to determinate the resonance with 10 Hz accuracy, i.e. the system has a 10 Hz accuracy

With regards to the amplitude of the resonance, this varies very quickly in few Hz close to the resonance frequency. Consequently, if the harmonic resonance matches up with the exact resonance frequency, the measured amplitude in the simulation will be bigger than in cases where the harmonics in the train are close to the exact frequency of the resonance. Thus, this analysis can measure accurately the frequency of the resonance, but not the amplitude, the amplitude is only an approximated value.

In the next step of the analysis, the influence of the cable length in the range of 20Km to 110Km is evaluated. The frequency response of the considered transmission system with this variation is shown in Figure 6.8.

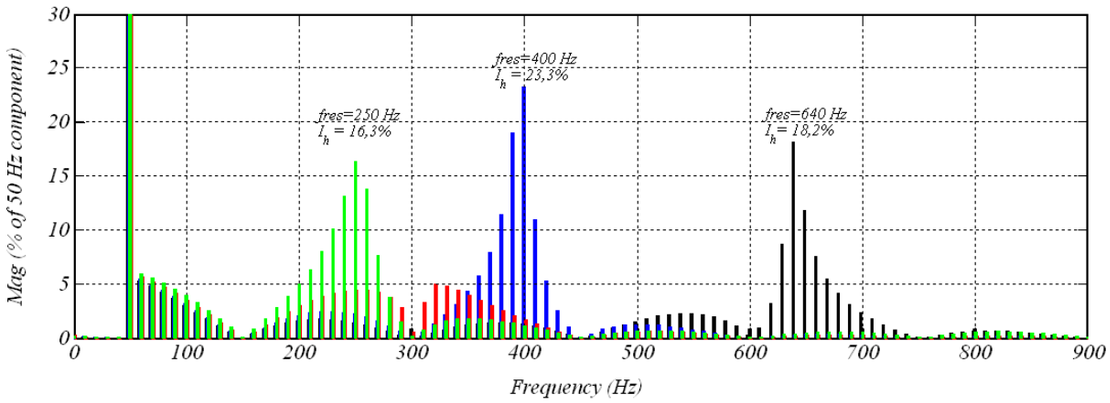

Figure 6.8 Frequency response of the transmission system varying the cable length from: 20Km (black), 50Km (blue), 80Km (green) and 110Km (red).

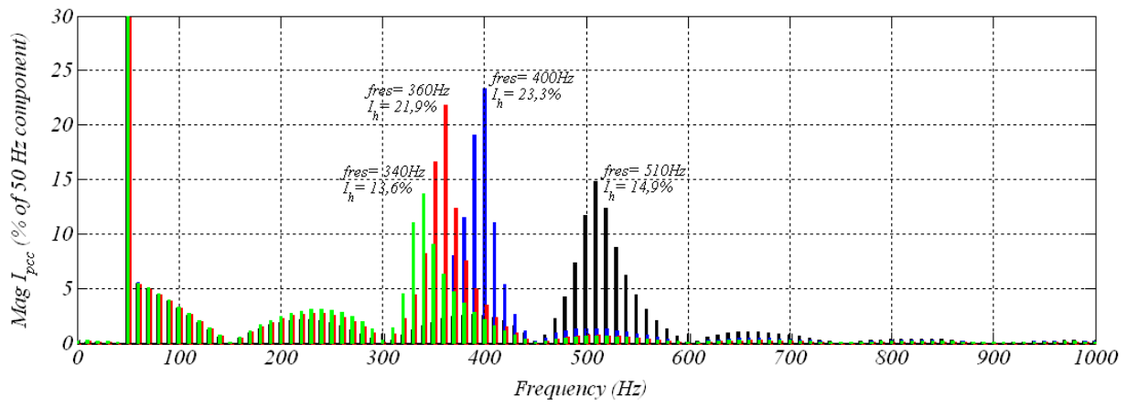

Figure 6.9 Frequency response of the transmission system varying the short circuit impedance from: 2 % (black), 5 % (blue), 8 % (green) and 11 % (red).

In this case, as the submarine cable length increases, the resonance frequency decreases. Note that the resonance of the transmission system with 80Km cable disappears, because in this case also all the multiples of the 3rd order harmonics cannot trespass the transformer.

In the third and last case there are considered different values for short circuit impedances. This variation is from the 2 % to 11 %, the simulation results are depicted in Figure 6.9.

In this last case, increasing the short circuit impedance decreases the resonance frequency, i.e. as in the two previous cases, increasing the inductive impedance or the capacitive impedance the frequency of the resonance decreases.

In the analyzed cases, the biggest variation is between 640Hz-250Hz, caused varying the cable length from 20Km to 110Km. However, in most of the cases the resonance is between 450Hz and 250Hz. In concordance with these results, in [109] is highlighted that AC transmission systems in conjunction with step-up transformer of the offshore substation, present the risk to amplify harmonics at low frequencies (inherently 3rd, 5th and 7th order harmonics).

6.4 Frequency response of the transmission system via analytic calculus

The objective of this section is to estimate the main resonance frequency in a simple and accurate way, alternatively to the method described in the previous section. Thus this section studies the calculation of the first resonance frequency of the transmission system, which is the main characteristic of the frequency response, using two different analytic ways.

To characterize in an easy way the main resonance frequency, with a potential risk of harmonic amplification, in [65] is presented a simple method. This approximation only takes into account the capacitive component of the submarine cable, neglecting the resistive and inductive components. In this way, it is possible to simplify the whole transmission system as an equivalent RLC circuit. Then, the resonance frequency of this simplified RLC circuit serves to approximate the resonance of the transmission system.

The second method uses state-space equations to estimate the resonance frequency of the transmission system. These equations take into account all the components of the cable and the short circuit impedance of the main grid, with the advantage that is not too more complicated than the first method.

Finally, to validate these two methods, the results obtained via analytic calculus are compared with the results obtained in simulation with PSCAD as described in section 6.3.2.

6.4.1 Frequency response of the transmission system via state space equations

6.4.1.1 State space equations for the transmission system with a cable modeled with a unique "π" circuit

At first, in order to explain with an example the method of the state-space equations, the simplest case is analyzed. The step-up transformer is considered as an equivalent inductance and the main grid as an ideal voltage source with short circuit impedance.

With regards to the submarine cable, this is modeled using several "π" circuits in series, (see section 4.2.2.2.4). This model has a frequency limit to represent the cable, i.e. the cable model has a valid range in frequency, out of this frequency range, the cable model and as a result the state-space equations cannot be used, since the error becomes too high. For the simplest case, the present case, the cable is modeled as a unique "π" circuit (N=1).

Once the equivalent circuit in impedances of the considered model is determined, it is possible to obtain the frequency response applying the state-space equations, the procedure is as follows:

In the first step, the names and the directions for all the currents of all the branches of the circuit are established as illustrated in, Figure 6.10.

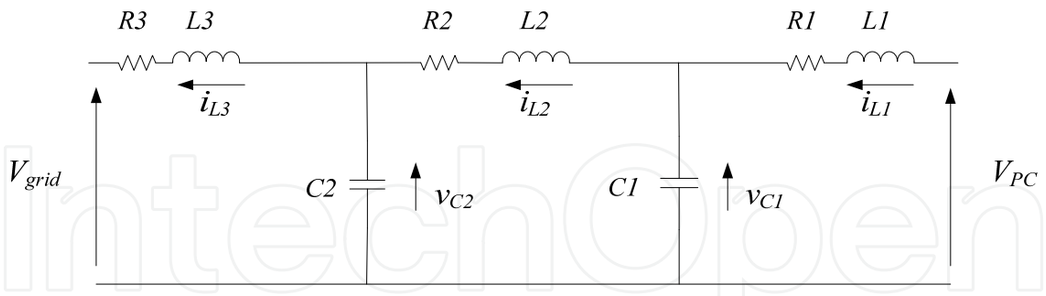

Figure 6.10 Single phase representation of the transmission system with the submarine cable modeled as a unique "π" circuits.

Where: *L1* represents the equivalent inductance of the step-up transformer, *R1* represents the equivalent resistance of the step-up transformer, *R2* represents the resistive part of the submarine cable, *L2* represents the inductive part of the submarine cable, (*C1*=*C2*) represent the capacitive part of the submarine cable and (*L3* and R3) represent *Lsc* and *Rsc* respectively, short circuit impedances.

In the second step, the differential equations for the currents in inductances and for voltages in capacitors are obtained, equations (131) - (135).

$$\frac{di_{L1}}{dt} = \frac{1}{L1} \cdot \left(\mathrm{V}_{PC} - v_{C1} - i_{L1} \cdot R1 \right) \tag{131}$$

$$\frac{dv_{C1}}{dt} = \frac{1}{C1} \cdot \left(i_{L1} - i_{L2} \right) \tag{132}$$

$$\frac{di_{L2}}{dt} = \frac{1}{L2} \cdot \left(v_{C1} - v_{C2} - i_{L2} \cdot R2 \right) \tag{133}$$

$$\frac{dv_{C2}}{dt} = \frac{1}{C2} \cdot \left(i_{L2} - i_{L3} \right) \tag{134}$$

$$\frac{di_{L3}}{dt} = \frac{1}{L3} \cdot \left(v_{C2} - V_{grid} - i_{L3} \cdot R3 \right) \tag{135}$$

Looking at equations (131) - (135), the variables of the differential equations i_L and v_C are independent. In the same way, these variables represent independent physical elements, so, those variables are state space variables.

Thus, if these equations are written in matrix notation (equation (137)), the state-space matrix is obtained as follows:

$$\dot{x} = Ax + Bu \tag{136}$$

$$d/dt \cdot \begin{bmatrix} i_{L1} \\ v_{C1} \\ i_{L2} \\ v_{C2} \\ i_{L3} \end{bmatrix} = \begin{bmatrix} -R1/L1 & -1/L1 & 0 & 0 & 0 \\ 1/C1 & 0 & -1/C1 & 0 & 0 \\ 0 & 1/L2 & -R2/L2 & -1/L2 & 0 \\ 0 & 0 & 1/C2 & 0 & -1/C2 \\ 0 & 0 & 0 & 1/L3 & -R3/L3 \end{bmatrix} \cdot \begin{bmatrix} i_{L1} \\ v_{C1} \\ i_{L2} \\ v_{C2} \\ i_{L3} \end{bmatrix} + \begin{bmatrix} 1/L1 & 0 \\ 0 & 0 \\ 0 & 0 \\ 0 & 0 \\ 0 & -1/L3 \end{bmatrix} \cdot \begin{bmatrix} \mathrm{V}_{PC} \\ V_{grid} \end{bmatrix} \tag{137}$$

Finally, the poles or eigenvals of the system are calculated (from *A* matrix), to determine its resonance frequency.

6.4.1.2 State space equations for the transmission system with a cable modeled with N "π" circuits

In the next step forward of the analysis, the procedure explained in the previous section (6.4.1.1) is applied to a generic case where the transmission system has a cable modeled with N "π" circuits, Figure 6.11.

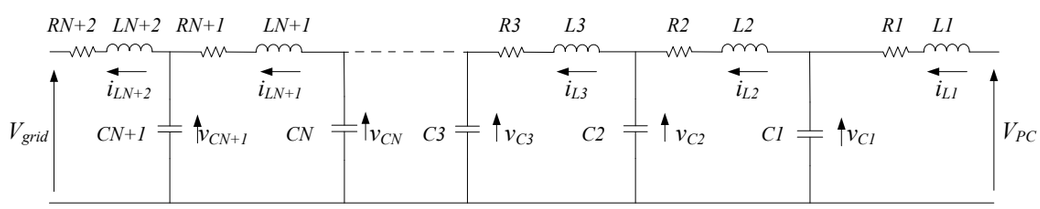

Figure 6.11 Single phase representation of the transmission system with the submarine cable modeled as N "π" circuits.

Where: *L1* represents the equivalent inductance of the step-up transformer, (*R2=R3=…=RN+1*) represent the resistive part of the submarine cable, (*L2=L3=…=LN+1*) represent the inductive part of the submarine cable, (*C1* to *CN+1*) represent the capacitive part of the submarine cable and (*LN+2* and *RN+2*) represent *Lsc* and *Rsc* respectively, short circuit impedances.

For the generic transmission system, following the procedure explained in the previous section, the state-space variables are defined and the estate-space equations are obtained. These state-space equations in matrix notation are displayed in equation (138). The reader can find the similarities of the matrix structure in expressions (137) and (138).

$$d/dt\cdot\begin{bmatrix} i_{L1} \\ v_{C1} \\ i_{L2} \\ .... \\ i_{LN+1} \\ v_{CN+1} \\ i_{LN+2} \end{bmatrix} = \begin{bmatrix} -R1/L1 & -1/L1 & 0 & .... & 0 & 0 & 0 \\ 1/C1 & 0 & -1/C1 & .... & 0 & 0 & 0 \\ 0 & 1/L2 & -R2/L2 & .... & 0 & 0 & 0 \\ .... & .... & .... & .... & .... & .... & .... \\ 0 & 0 & 0 & .... & -RN+1/LN+1 & -1/LN+1 & 0 \\ 0 & 0 & 0 & .... & 1/CN+1 & 0 & -1/CN+1 \\ 0 & 0 & 0 & .... & 0 & 1/LN+2 & -RN+2/LN+2 \end{bmatrix} \cdot \begin{bmatrix} i_{L1} \\ v_{C1} \\ i_{L2} \\ .... \\ i_{LN+1} \\ v_{CN+1} \\ i_{LN+2} \end{bmatrix} + \begin{bmatrix} 1/L1 & 0 \\ 0 & 0 \\ 0 & 0 \\ .... & .... \\ 0 & 0 \\ 0 & 0 \\ 0 & -1/LN+2 \end{bmatrix} \cdot \begin{bmatrix} V_{PC} \\ V_{grid} \end{bmatrix} \quad (138)$$

6.4.1.3 Frequency response of the transmission system via state space equations

Finally, the frequency response of the transmission system with the submarine cable, the step-up transformer and the main grid of the previous section (Table 4.3, Table 6.4 and Table 6.5) via state-space equations is obtained.

For the submarine cable model, 10 "π" circuits in series are considered. In this way, the cable model is composed by sufficient "π" circuits to make possible the representation of the submarine cable in the correct frequency range, i.e. sufficient to represent correctly the cable until the resonance. In more detail, with 10 "π" circuits it is possible to represent the submarine cable in a valid range for all the resonances analyzed in the previous section [54] ,by means of equation (139).

$$f_{\max} = \frac{Nv}{8l} = \frac{N}{8\cdot l\cdot\sqrt{LC}} = \frac{10}{8\cdot 110\cdot\sqrt{0.352\cdot 0.233\cdot 10^{-9}}} = 1250\,Hz \Rightarrow 7884\,rad/s \quad (139)$$

If the resonance frequency estimated in this way is out of the cable model valid range, it is not valid and the analysis must be repeated with a valid cable model.

Finally, applying the developed generic equation (138), to the considered transmission system, the frequency response depicted in Figure 6.12 is obtained.

As can be observed in Figure 6.12, the first resonance of the system is located at 388 Hz, very close to the 400 Hz estimated via PSCAD simulation. With regards to the amplitude of the resonance, in this case also is an approximation, due to the fact that the calculus is based on a model with lumped parameters, not in a model with distributed parameters which is more accurate.

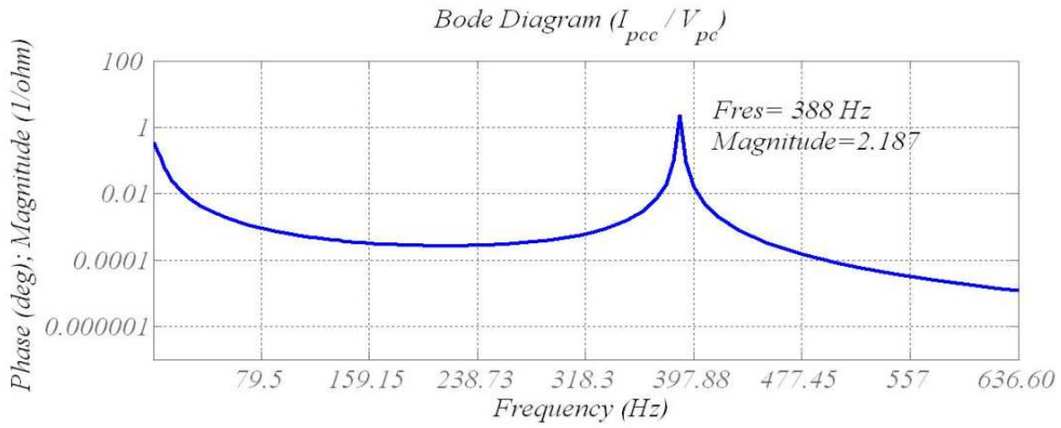

Figure 6.12 Frequency response of the transmission system with the cable modeled as 10 "π" circuits in series using state space equations.

6.4.2 Simplified method avoiding the inductive part of the submarine cable

The other method used to compare with the state-space equations is the simplified RLC method, described in [109]. Thus, a comparative is performed comparing the resonance frequency estimated with these three methods for different transmission system. Similarly as done in section 6.3.3, but in this case, the analysis only varies the cable length and the equivalent inductance of the step-up transformer.

The short circuit impedance of the main grid is not taken into account because the simplified RLC method does not consider it. The resonance frequency for the simplified RLC method of [109] is estimated with the following equation (140).

$$f_{\mathrm{Re}sonance} = \frac{1}{2 \cdot \pi \cdot \sqrt{\left(L_{Transformer} + L_{Cable}\right) \cdot C_{Cable}}} \tag{140}$$

6.4.3 Comparison and validation of the frequency response via state space equations

The objective of this section is to validate the state-space equations based method to estimate the first resonance. For that purpose, a comparative of three different methods is carried out. The method based on PSCAD simulation with the validated cable is considered as the most accurate method.

Hence Table 6.6, summarizes the obtained resonance frequencies varying the equivalent inductance of the step-up transformer for the considered three methods. The variation of the equivalent inductance is the same of the section 6.3.3. (3% to 12%).

Transformers L	*3 %*	*6 %*	*9 %*	*12 %*
PSCAD simulation	*450*	*400*	*370*	*350*
State space equations	*453,6*	*388,3*	*356,5*	*339*
Simplified RLC	*264,75*	*218*	*190,9*	*171,4*

Table 6.6 Comparative of the results obtained for the variation of the equivalent inductance of the step-up transformer.

To verify the state-space equations method at different conditions, a second comparative is carried out. In this second case, the cable length is varied, yielding the resonances depicted in Table 6.7

Cable length (Km)	*20*	*50*	*80*	*110*
PSCAD simulation	*640*	*400*	*300*	*250*
State space equations	*631,8*	*388,3*	*297,6*	*246,6*
Simplified RLC	*392*	*218*	*156,67*	*124,8*

Table 6.7 Comparative of the results obtained for the variation of the cable length.

Looking at Table 6.6 and Table 6.7, it can be concluded that the state-space equation method is a good approximation for estimating the resonance frequency, even under different transmission conditions options.

On the other hand, the simplified RLC method does not provide as accurate results as expected to characterize the resonance frequency. However it could be useful to obtain a very simplified and first approximated value.

6.5 Frequency response of the offshore wind farm

As is distinguished in chapter 3, the electric infrastructure of the offshore wind farm's connection is divided into two parts: The transmission system and the inter-turbine grid. The frequency response of the transmission system has been already characterized in previous section, therefore, the next step consist on characterizing the frequency response of the entire electric infrastructure, including the inter-turbine grids. Thus, this second part of the analysis is mainly focused on the inter-turbine grid and its characteristics.

The equivalent impedance of an offshore wind farm varies with changes in the configuration of the inter-turbine grid. As a result, the frequency response of the system varies as well. Thus, the frequency response of the wind farms for different configurations have to be investigated separately [25].

Consequently, based on the transmission system evaluated in section 6.3.2 the analysis performed in this section is focused on the effect of different aspects of the wind farm, like: number of feeders (or radials) in the inter-turbine grid or the location of each wind turbine. The analysis is made from the viewpoint of the wind turbine, which is considered the potential harmonic source in normal operation.

Without the appropriate models is not possible to estimate the resonances of the system. Therefore, the base scenario defined in chapter 5 is used.

This scenario presents a radial design for the inter-turbine grid, where each one of those radials is composed by 6 wind turbines of 5MW. The voltage level of the inter-turbine grid is medium voltage, 33kV. As regards to the spatial disposition of the wind turbines, there is considered as a rectangle (see section 3.3), Figure 6.13.

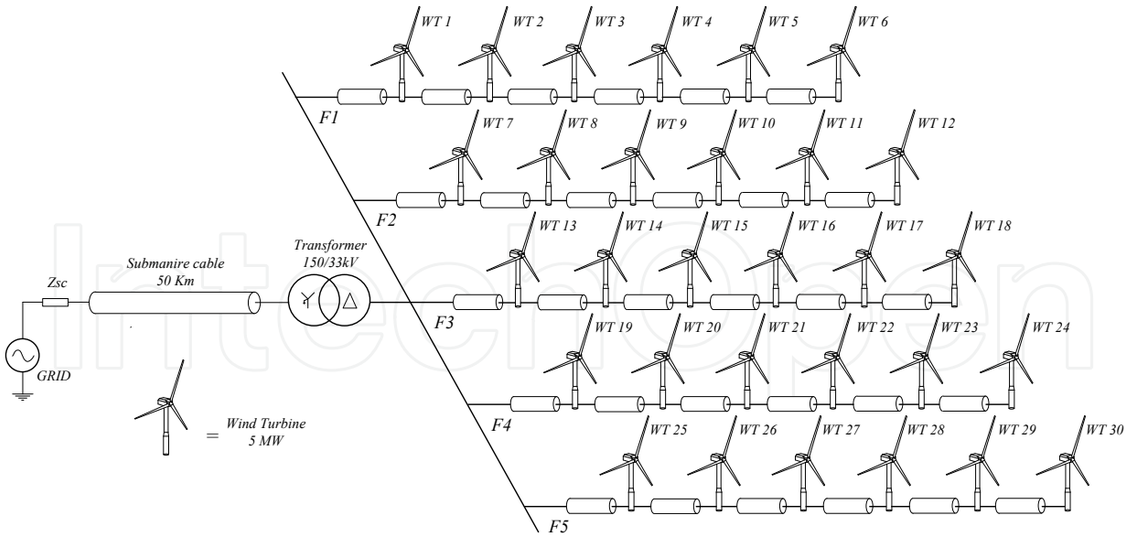

Figure 6.13 The lay-out of the offshore wind farm, which is the base of the resonances analysis.

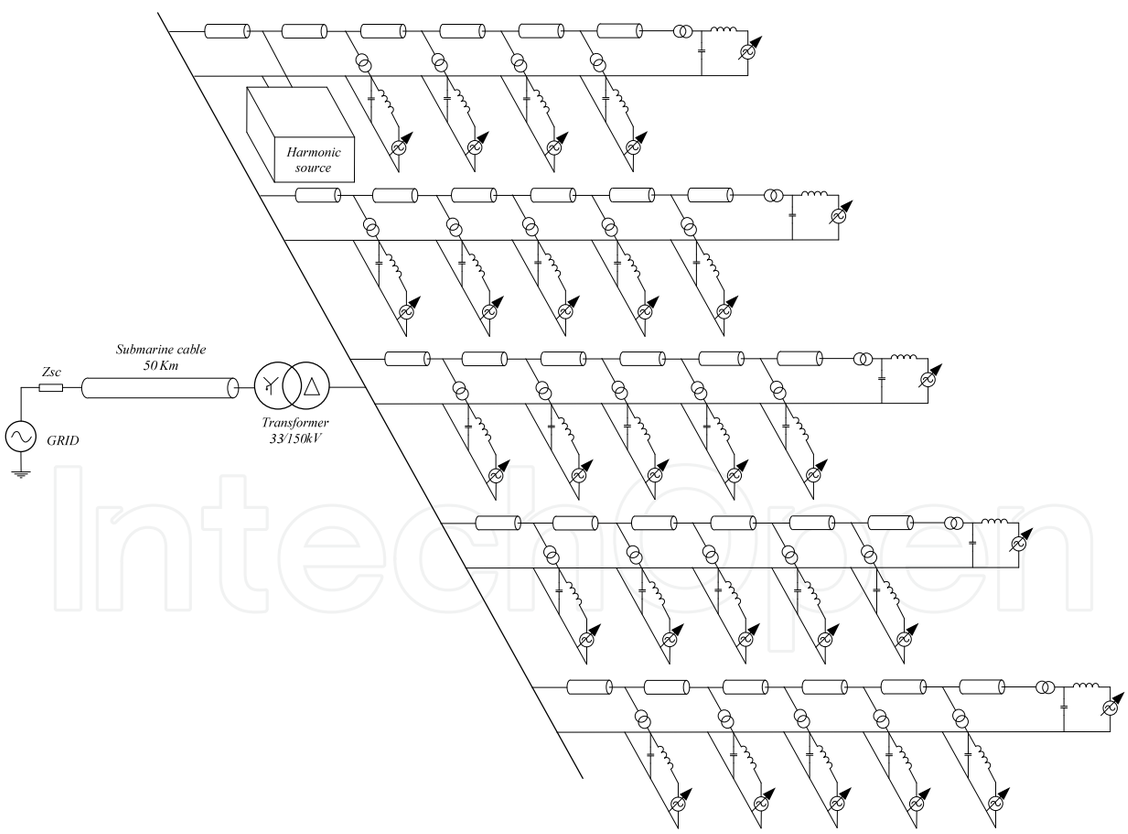

Figure 6.14 The simulation scenario of the offshore wind farm, which is the base for the frequency response analysis.

Considering that the transmission system is equal to the characterized in section 6.3.2, the last feature to define the whole offshore wind farm is the inter-turbine submarine cable. Hence, as inter-turbine submarine cable an ABB XLPE cable with the adequate nominal voltage and power is chosen. The characteristics of this cable are shown in Table 5.21, chapter 5.These characteristics are filled into the PSCAD template, for the model explained in section 4.2.3 with the corrections exposed in section 4.2.4.

The aim of this evaluation is to calculate the frequency response of the entire electric connection infrastructure. Thus, the wind turbine model is not considered as a key issue.

Therefore, the wind turbines are considered as an ideal controlled voltage source with a LCL filter, (see section 5.2.2.3). The filter used to connect the wind turbine to the local inter turbine grid, Figure 6.14.

Taking the scenario depicted in Figure 6.14 as base to estimate the frequency response, the same procedure of section 6.3.2 is used. In this way, to know the frequency response for a specific wind turbine, it is substituted by a harmonic voltage generator (Figure 6.14), which generates a harmonic train in the frequency range of 50Hz-5000Hz, Figure 6.3.

6.5.1 Frequency response of a wind turbine depending on its position in the inter-turbine network

Looking at Figure 6.13, it is possible to observe how from the viewpoint of each wind turbine, the equivalent impedance seen is different depending on its location in the inter-turbine grid, i.e. there is not the same equivalent impedance at the output of the 25th wind turbine and at the output of the 30th wind turbine.

To quantify the variation of the frequency responses of each wind turbine, in this section the frequency responses for all the wind turbines of a feeder are estimated. To perform this evaluation, the harmonic voltage source is placed in different positions of the feeder (or radial) and for each position the signals at the PCC are measured. Then, applying the FFT to the signals of the PCC, it is possible to estimate the frequency response for each individual wind turbine.

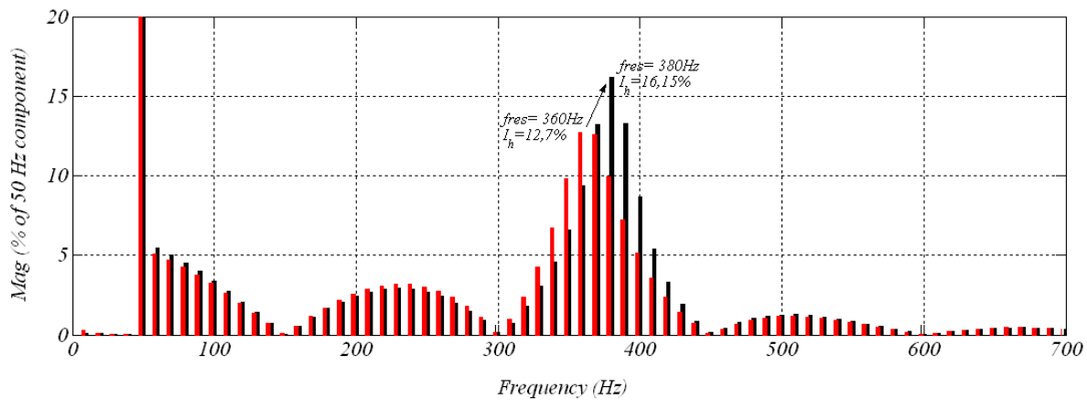

Figure 6.15 Harmonic currents at the PCC depending on the location of the harmonic voltage source inside the inter turbine grid. Substituting the 30th wind turbine (red) and substituting the 25th wind turbine (black).

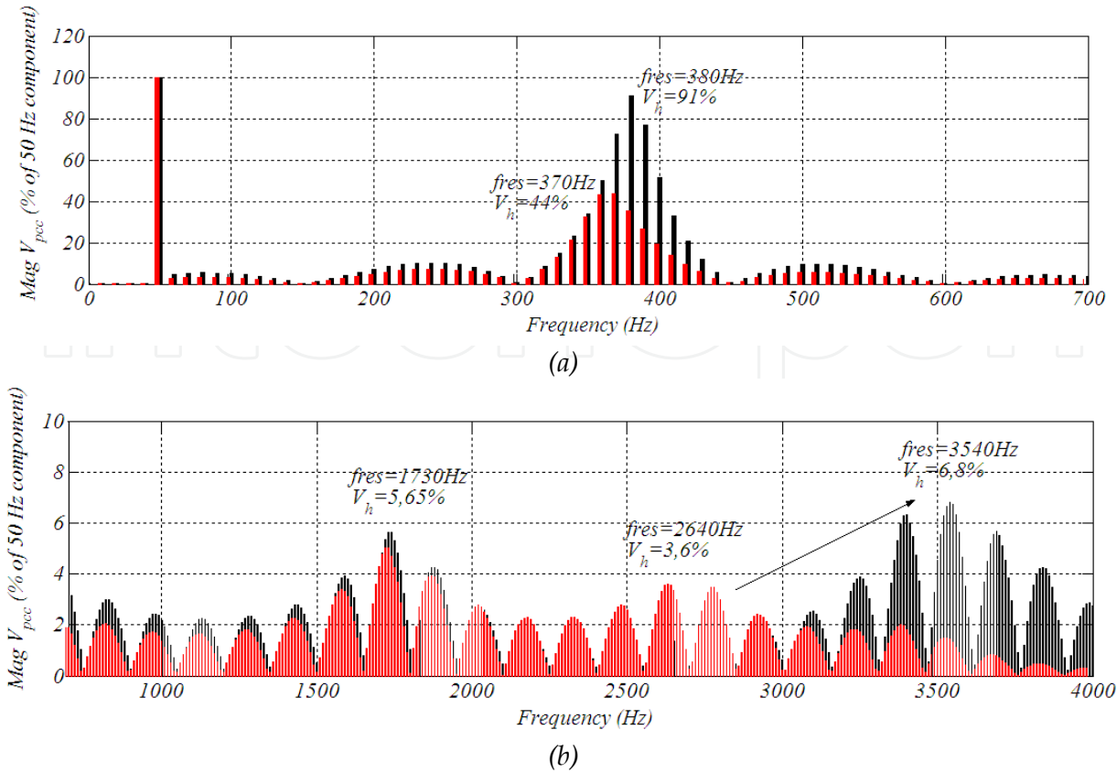

Figure 6.16 Harmonic voltages at the PCC depending on the location of the harmonic voltage source inside the inter turbine grid. Substituting the 25th wind turbine (black) and substituting the 30th wind turbine (red): (a) more detail in the main resonance and (b) more detail in high frequencies.

In the first evaluation, the frequency response of each wind turbine is obtained from the 25th to the 30th. The results for the harmonic currents are depicted in Figure 6.15 and the results for harmonic voltages are depicted in Figure 6.16.

The frequency response of the whole system is similar to the frequency response of the transmission system only. However, the resonance frequency has a short variation. The transmission system presents the resonance at 400 Hz (section 6.3.2, Figure 6.5), but as can be seen from Figure 6.15, the frequency response from the wind turbine viewpoint depends on each wind turbine and is located in the range of 360-380 Hz, close to the 400Hz but not the same.

As seen in section 6.3.3, the step-up transformer does not allow to transmit 3rd order harmonics and multiples. Looking to the results for the 30th wind turbine, the harmonics located at 360Hz and 370Hz have similar amplitudes in both cases (current and voltage), probably the resonance is between them. This fact, can explain the notorious amplitude reduction.

Applying the FFT to the voltage at PCC (Figure 6.16), it is possible to see other two more "small resonances" (attenuated frequencies, but less than the rest), besides the transmission system's resonance.

The first one of these two frequency groups less attenuated than the rest is located between the 1500Hz and 2000Hz. This small resonance has not variations, i.e. is independent to the location of the wind turbine. However, the second group of these frequencies less attenuated depends on the location of the wind turbine. Thus, depending on the location of the wind turbine, the "small resonance" can be around 2500Hz or 3500Hz. The closer is placed the wind turbine to the offshore substation (shorter cable length to the collector point, and less impedance), bigger is the frequency of the resonance.

Note that these two "small resonances" have significantly smaller amplitude than the main resonance at (360Hz-380Hz).

6.5.2 Frequency response of the offshore wind farm depending on the feeders in its inter-turbine network

In the first scenario described in section 6.5, 5 feeders (F1-F5) of 6 wind turbines each one are considered, Figure 6.13. However, the internal impedance of the wind farm can have variations with configuration changes, like changes in the number of feeders.

Thus, in this section the frequency response for different inter-turbine grid configurations is evaluated. Inter turbine grids with 2 feeders (F1 and F2) to 5 feeders (F1-F5), Figure 6.13 are considered, maintaining the same number of wind turbines for each radial, not the total number of wind turbines of the wind farm.

In this case, the harmonic voltage source is placed at the first wind turbine of each feeder (7, 13, 19 or 25, Fig. 15), because at this point, the second "small resonance" is closer to the fundamental frequency than in any other location of the feeder, Figure 6.16 (b). The simulation results (FFT of the current and voltage at the PCC) for the considered configurations are depicted in Figure 6.17 and Figure 6.18

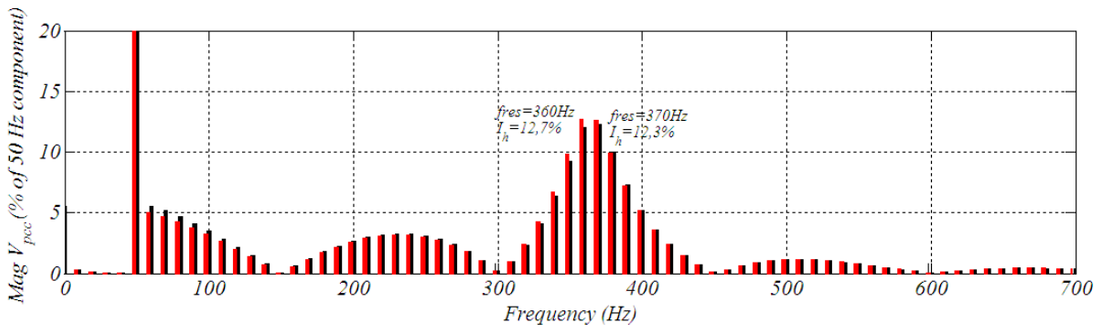

Figure 6.17 Harmonic currents at the PCC depending on the number of feeders in the inter-turbine grid. With 2 feeders F1-F2 (black) and with 5 feeders F1-F5 (red).

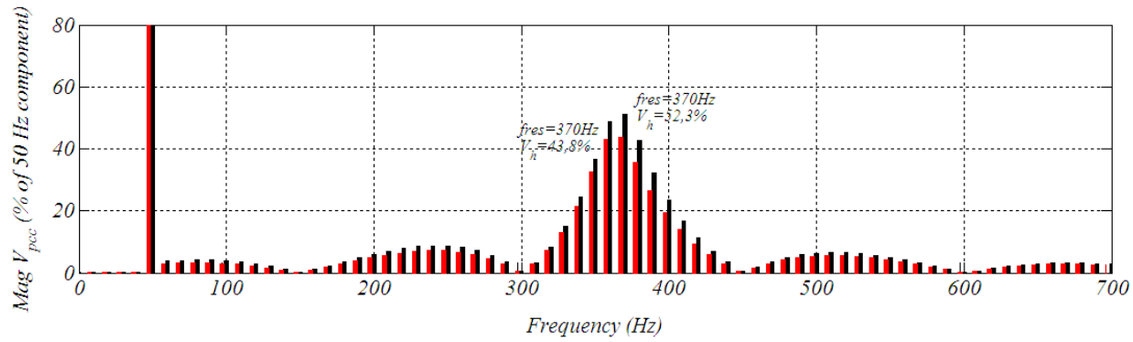

(a)

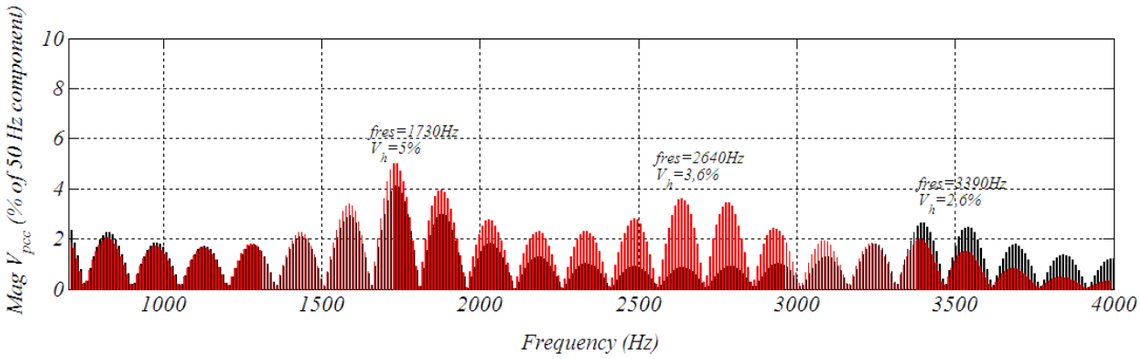

(b)

Figure 6.18 Harmonic voltages at the PCC depending on the number of feeders in the inter-turbine grid. With 2 feeders F1-F2 (black) and with 5 feeders F1-F5 (red).

From the evaluation of the results of Figure 6.17, it is possible to determine that the first and main resonance of the system have not big variations for different configurations of the local inter-turbine grid. However, the second of the "small resonances" (frequency groups less attenuated) varies with these configuration changes. If there are fewer feeders, the second "small resonance" occurs at higher frequencies.

6.5.3 Frequency response of the offshore wind farm depending on the number of feeders for each step-up transformer's primary

In order to take into account cases where the offshore wind farm have a step-up transformer in the offshore substation with more primary windings than one, the present section analyzes an inter-turbine network configuration with two primary windings, as depicted in Figure 6.19. The purpose of the analysis is to know how affects this extra primary winding to the frequency response of the offshore wind farm.

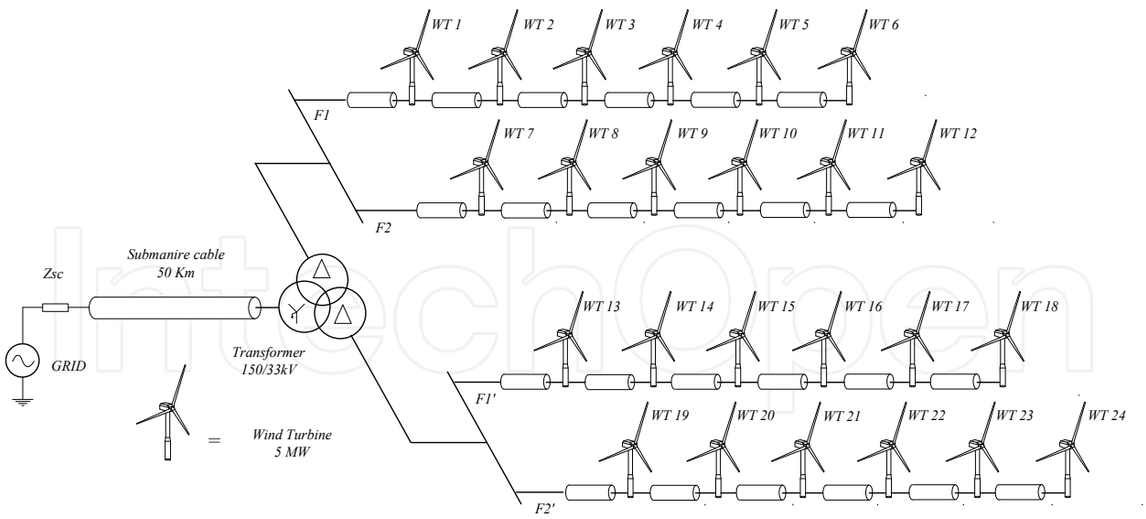

Figure 6.19 Simplified scheme of the simulation scenario of the offshore wind farm with two primary windings.

To know the influence of the extra winding, the results of the configuration depicted in Figure 6.19 and the configuration depicted in Figure 6.13 with only two feeders, are compared. The comparison these frequency responses are served Figure 6.20 And Figure 6.21.

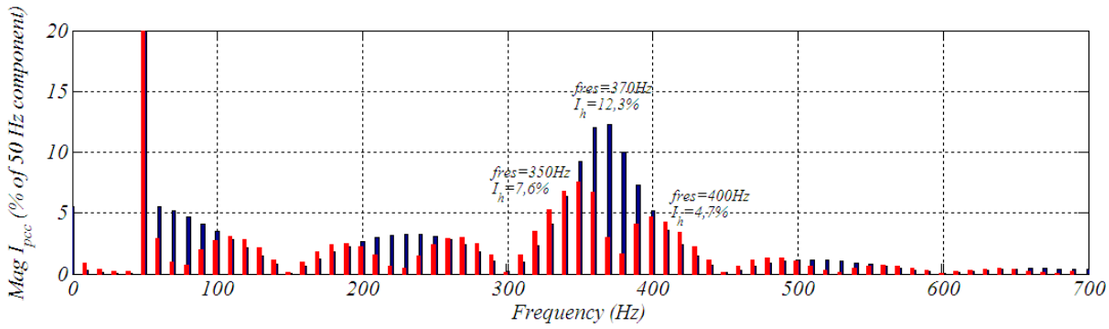

Figure 6.20 Harmonic currents at the PCC. With 2 feeders F1-F2 (red) and with 2 feeders on each primary winding F1-F2 and F1'-F2' (black).

Looking at the results in Figure 6.20, it is possible to see that the use of two windings connected as delta-star(grounded)-delta, where the secondary windings have delta connection, does not allow to transmit multiples of 3rd order divided by two harmonics (multiples of 150Hz/2, 75 Hz) to the PCC. As a result, the frequency response of the system from the viewpoint of the wind turbine presents less harmonic components.

However, as can be seen in Figure 6.21 (b), for the voltage harmonics, there is a new group of frequencies less attenuated at 2520 Hz.

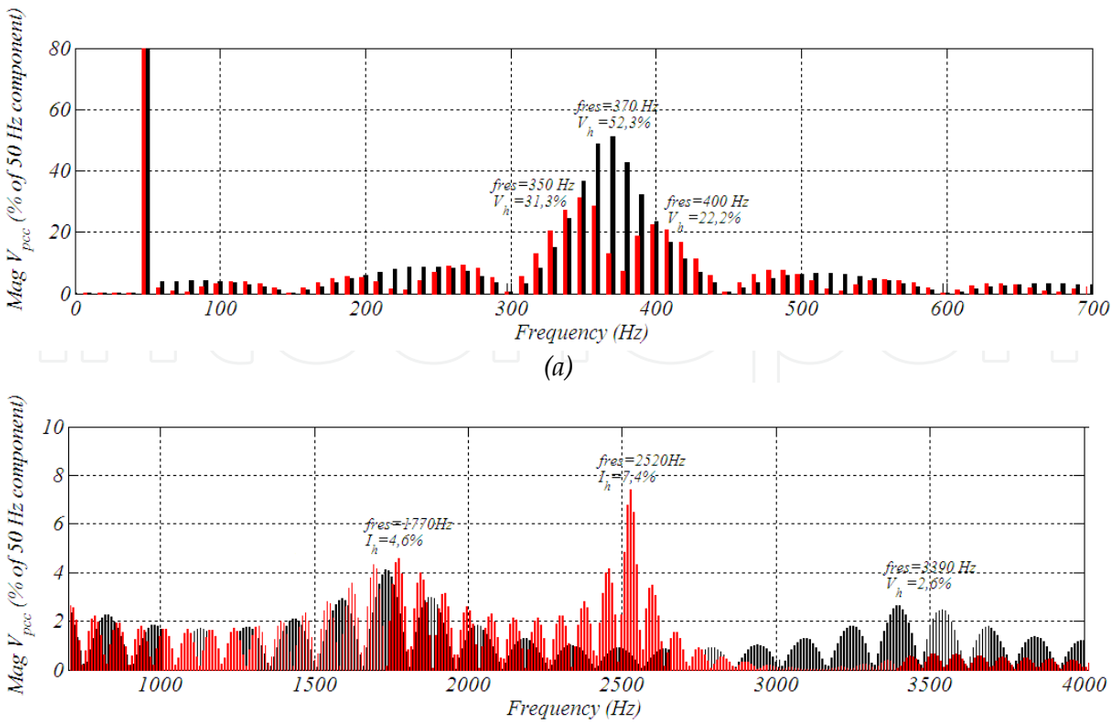

Figure 6.21 Harmonic voltages at the PCC. With 2 feeders F1-F2 (black) and with 2 feeders on each primary winding F1-F2 and F1'-F2' (red).

6.6 Harmonic risk evaluation for the considered base scenario

In the previous section, an evaluation of the frequency response of the electric connection infrastructure is carried out. In the next step forward, a specific case for the base scenario considering equivalent wind turbines is analyzed.

The control strategy implemented in the grid side converter of the wind turbine has a notorious influence in the harmonic components injected to the electric connection infrastructure. As is defined in chapter 5, at the grid side converters, a vector control with two current loops is considered, one for the quadratic component and the other for the direct component, in order to control independently both of them. As regards to the modulation, a PWM modulation is used.

As is mentioned before, the simulation of a scenario with 30 complex wind turbine models can be computationally unviable. Thus, starting to the scenario described in chapter 5, a model with an equivalent wind turbine of 30 MW for each radial is developed. As says [110], using N equivalent wind turbines it is possible to have reasonable accurate representation of an offshore wind farm made up with N radials. Thus, the new scenario with wind turbine models is depicted in Figure 6.22.

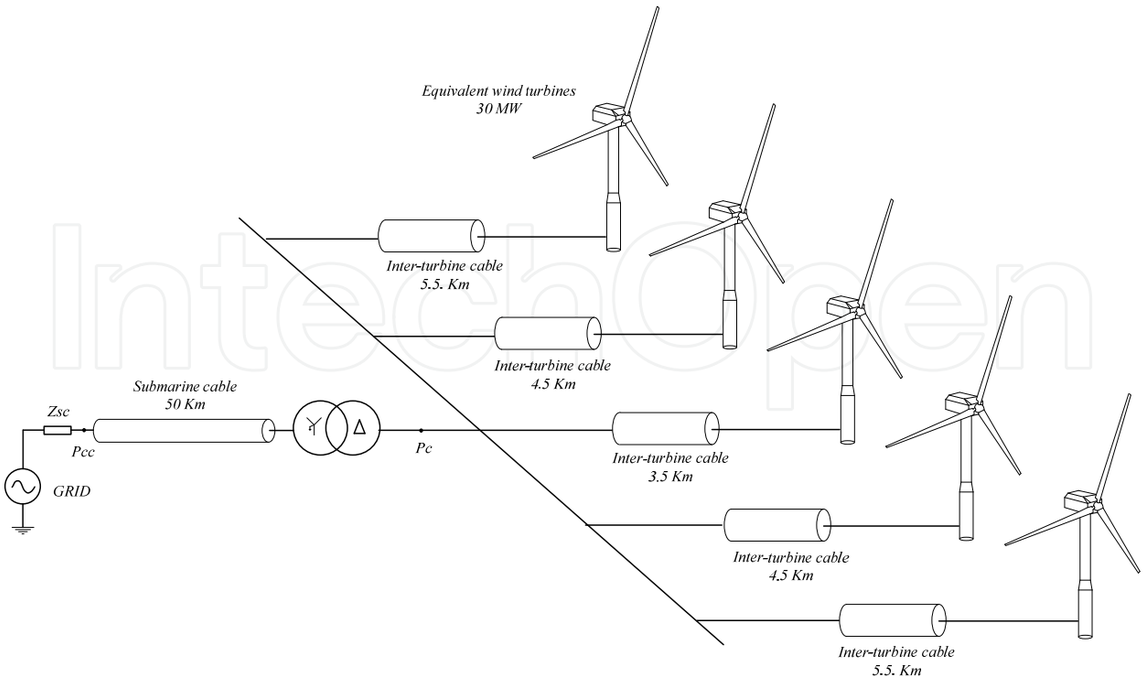

Figure 6.22 Diagram of the simulation scenario with wind turbine models.

To verify that the connection infrastructure of the equivalent simulation scenario has a similar frequency response to the entire offshore wind farm, the frequency response of the equivalent wind farm is obtained via PSCAD. So, using the same procedure of the sections 6.3 and 6.5, an equivalent wind turbine is substituted by a harmonic voltage source (same harmonic train Figure 6.2) and the FFT of the signals is carried out in the PCC, Figure 6.23.

Making out a comparison between both frequency responses, it is possible to verify that the equivalent offshore wind farm and the whole wind farm have a similar frequency response in steady-state.

Thus, comparing the frequency response of the equivalent wind farm (Figure 6.23) with the frequency response of the entire wind farm (Figure 6.15 and Figure 6.16), can be seen how they have roughly the same frequency response.

Finally, the maximum harmonic levels allowed in the main grid for this specific scenario are defined. According to the IEEE-519 standard, for a short circuit impedance of 5% and a 150kV, these limits are as follows, Table 6.8

IEEE-519 Harmonic limits for voltage and current

I_{SC}/I_L	n < 11	11 ≤ n ≤ 17	17 ≤ n ≤ 23	23 ≤ n ≤ 35	35 ≤ n	*THD*
20-50	3.5 %	1.75 %	1.25 %	0.5 %	0.25 %	4.0 %
			Individual harmonics		*THD*	
Above 161kV			*1.0 %*		*1.5 %*	

Table 6.8 Harmonic limits for voltage and current for the specifications of the simulation scenario.

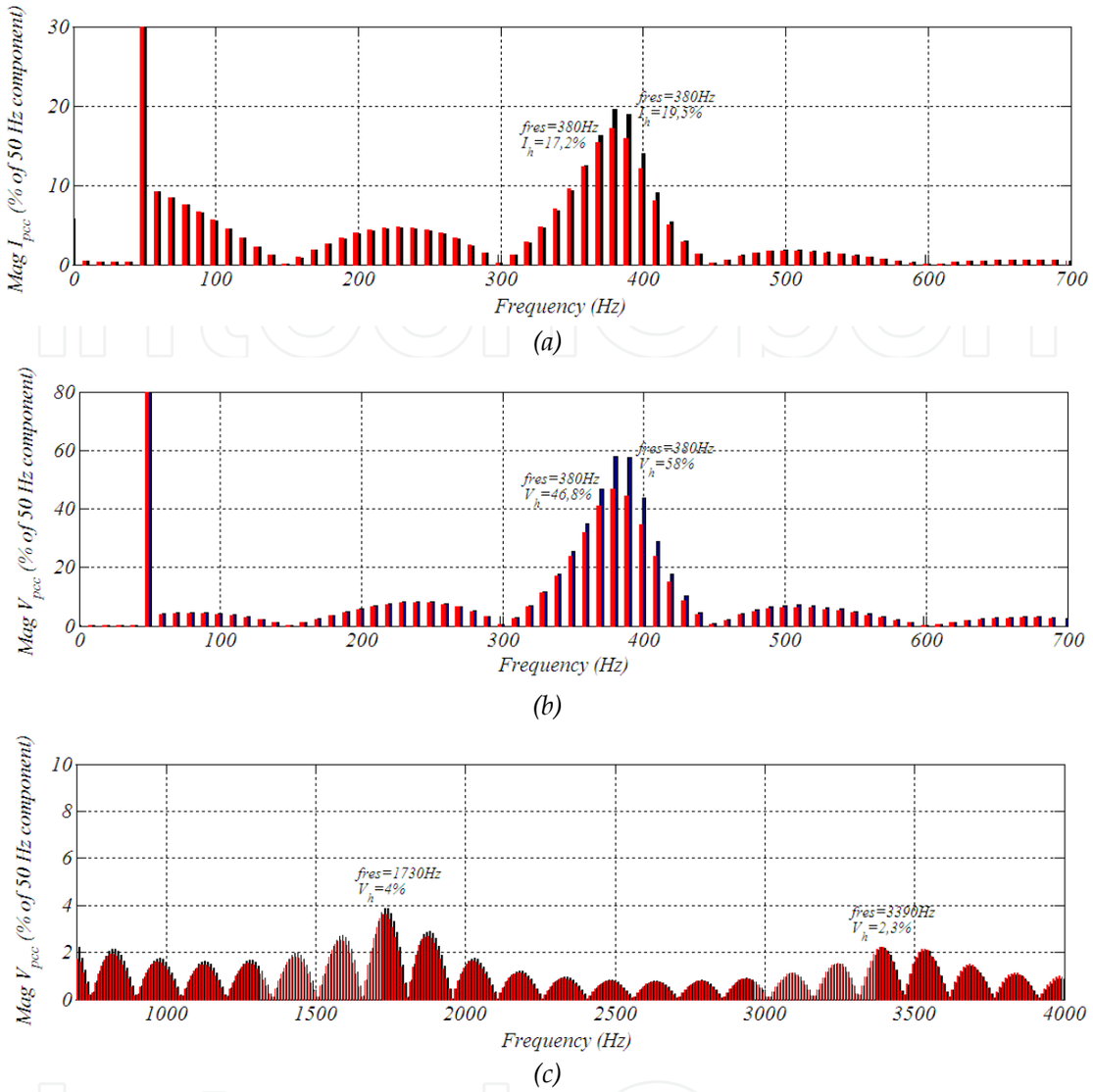

Figure 6.23 Frequency response of the equivalent wind farms model via PSCAD. Frequency response from the viewpoint of the equivalent wind turbine closest the collector point (red) and for the equivalent wind turbine 5.5 Km away the collector point (Blue). FFT of the current (a) and FFT of the voltage (b)-(c).

6.6.1 The output voltage of the considered wind turbines

In this section, the harmonic spectrum of the input voltage is characterized, i.e. defined all the harmonics generated by the wind turbines. In this way, the considered input voltage spectrum is based on a PWM modulation and a LC-L filter. The voltage generated in the grid side inverter (referenced to the neuter point) is shown in Figure 6.24.

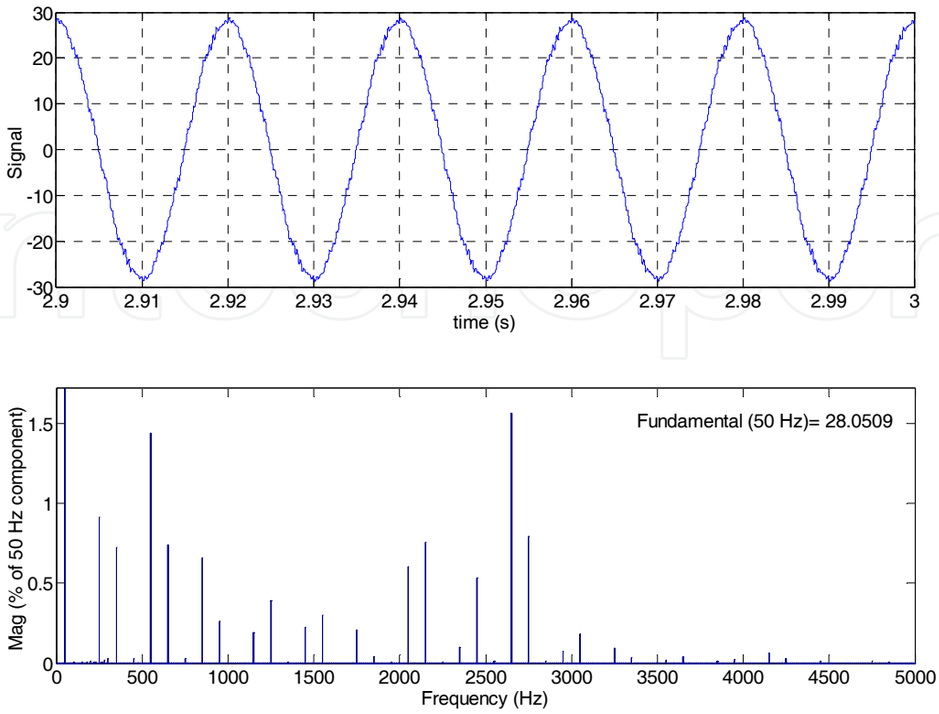

Figure 6.24 Voltage behind the connection filter of the grid side inverter and its frequency spectrum, while the equivalent wind turbine is generating the nominal power.

The voltage with the frequency spectrum off Figure 6.24 is one of the input voltages to the electrical connection infrastructure. For each one of the equivalent wind turbine is considered the same input voltage.

The frequency spectrum depicted in Figure 6.24 is used as an example (like a generic wave of a generic wind turbine) in the base scenario to perform an analysis of the harmonic risk.

So, considering this generic case as an example, it is possible to know how the different harmonics of each equivalent wind turbine interact with the electric connection infrastructure estimating via simulation the harmonic levels at the PCC.

The emitted harmonics for a specific wind turbine varies with the generated active power, at least with the considered control strategy. But, in the present analysis, only the harmonic levels on the PCC for the case while the wind farm is transmitting / generating the nominal power are estimated. This estimation is performed via PSCAD simulation of the scenario that is shown in Figure 6.22, the results are served in Figure 6.25 for current and in Figure 6.26 for voltage.

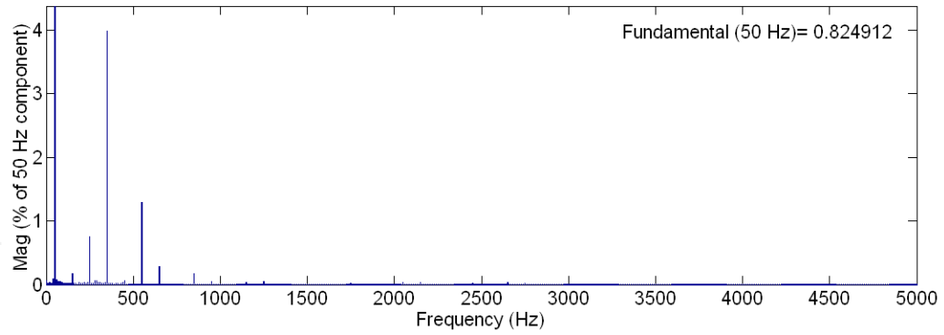

(f)

Figure 6.25 FFT of the current at the PCC for the base scenario while is transmitting / generating the nominal active power.

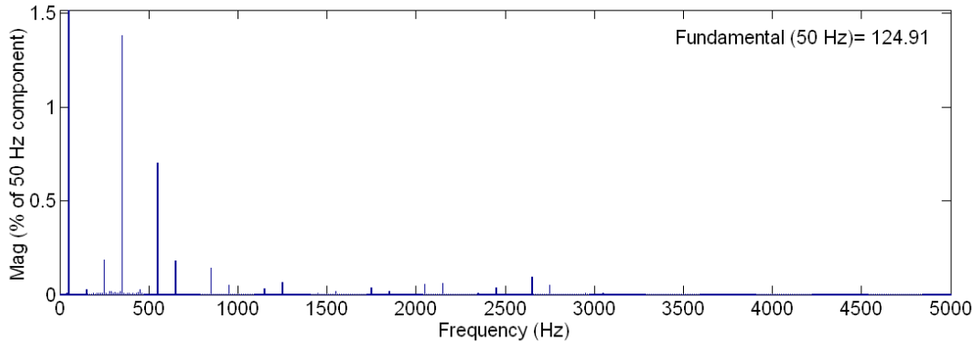

(f)

Figure 6.26 FFT of the voltage at the PCC for the base scenario while is transmitting / generating the nominal active power

Carrying out the FFT of the current and voltage at the PCC for the case while the wind farm is transmitting / generating the nominal power, Figure 6.25 and Figure 6.26, can be seen that the harmonic levels are bigger than the limit described in the standard IEEE-519 (Table 6.8), i.e. the harmonic levels at the PCC cannot fulfill the standard IEEE-519. The 350 Hz harmonic (Figure 6.25) is bigger than maximum amplitude allowed for a single harmonic at this point (<3.5%).

From Figure 6.25 and Figure 6.26, it is possible to observe two main harmonics (550Hz and 350 Hz) for current and voltage. The harmonic at 550 Hz is notorious in voltage and current, but this is the resonance frequency of the grid side inverter's connection filter, so it is not amplified by the electric connection infrastructure.

Finally, notice that the harmonic spectrum at the PCC is the combination of the voltage harmonic spectrum of the output voltage of the equivalent wind turbine (Figure 6.24) and the frequency response of the equivalent offshore wind farm (Figure 6.23).

Therefore, the 350 Hz harmonic component is amplified by the energy transmission system of the offshore wind farm. One solution to avoid this amplification caused by the transmission system is the use of resonant passive filters.

Resonant passive filters are based on accept or attract the harmonic current on a specific frequency to the filter branch. At this specific frequency, the RLC branch presents only the resistive part of the impedance, so, at this point the harmonic current is divided depending on the kirchoff law. Thus, the harmonic current is deviated depending on the relation between the impedance of the filter and the impedance of the circuit (see Appendix E: Resonant Passive Filters).

This means that the location of these filters determine the impedance of the circuit in parallel to it. So, the location of the resonant passive filters affects to the current that it is deviated by it.

Moreover, due to the fact that the harmonic currents are deviated to the passive filters, the passive filters do not reduce the harmonic distortion from the harmonic source to the passive filters. Therefore, to avoid the negative effects caused by the harmonics in the electric connection infrastructure (independently of the IEEE-519 standard fulfillment at the PCC) the passive filters have to be placed as close as possible to the harmonic source.

Another option is the use of active filters. Resonant passive filters, as their name describes, are made up exclusively with passive elements to remove a specific harmonic. On the contrary, the active power filters are made up with one or more inverters, usually voltage source inverters (VSI).

Basically, active power filters are made up by: a converter (usually VSI inverter), a device to storage energy (usually a capacitor), several circuits to measure current and voltage and a control circuit to generate the modulated reference signals to the converter. Besides these components, the active power filter can be provided by a transformer or a coil to connect the converter to the grid.

The main advantage of the active power filters in comparison with the passive filters is that they can be adapted to the changing conditions of the load and the electric grid.

Looking at the results displayed in Figure 6.15 and in Figure 6.16, it is possible to see that the main resonance of the system (350Hz) has not huge variations with variations in the configuration of the collector grid. Furthermore, in the present case, there are only two main harmonic frequencies at the PCC (Figure 6.26). So, due to its simplicity, in the present evaluation only passive filters are taken into account.

However, in the wind farm can be implemented many other solutions like active filters or control strategies oriented to mitigate harmonics.

6.6.2 Location of the passive filters in the transmission system

As is explained in the previous section, the location of the passive filters determines the impedance of the circuit in parallel to it and the current that it is deviated.

Therefore, in this section advantages and disadvantages to place these filters offshore and onshore are evaluated. Between both locations are some technical differences. For example, offshore side it is possible to connect the passive filter directly to a medium voltage grid, while onshore side only a high voltage grid is available.

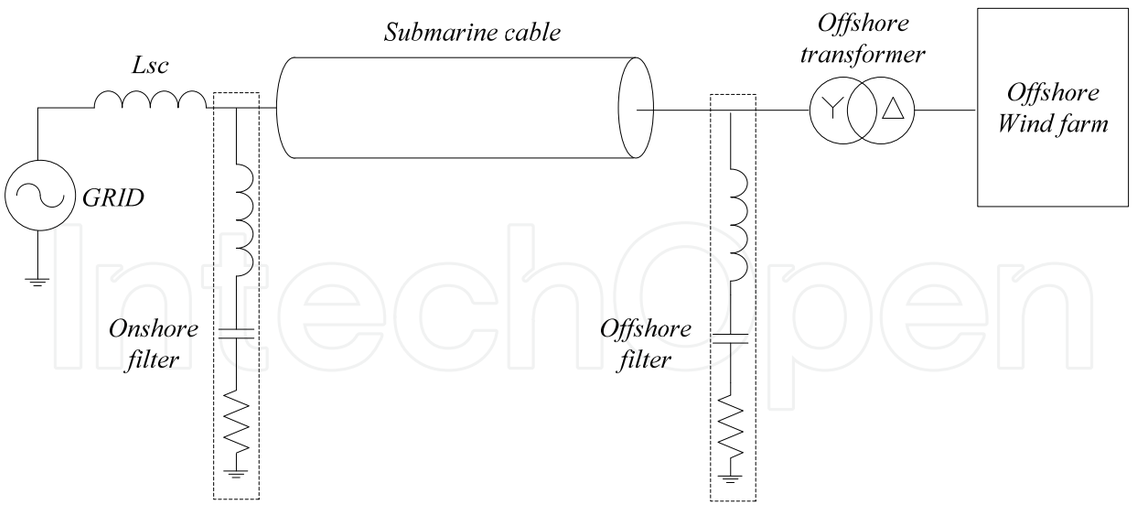

Figure 6.27 Transmission system with onshore and offshore RLC filters.

Nevertheless, in the present analysis, to see in a simple way the difference between these two locations, two identical equivalent filters connected to the same voltage (the transmission voltage 150 kV) are considered, Figure 6.27.

The RLC filters used in this comparative are tuned to filter the main harmonics detected in the PCC of the base scenario: 350 Hz and 550 Hz (Figure 6.25 and Figure 6.26). The characteristics of these filters are shown on Table 6.9.

	Fresonance=350 Hz	*Fresonance=550 Hz*
R	32.45 Ω	26.3 Ω
L	1.033 H	0.418 H
C	0.2 μF	0.2 μF
Δ*f*	5 Hz	10 Hz
Vn (50 Hz)	150 kV*	150 kV*
In (*fo*)	53.4 A	25 A

**Equivalent filters transformed to this voltage*

Table 6.9 Characteristics of the considered RLC filters.

Therefore, based on the scenario described in the previous section, the analysis of the best location for passive filters is carried out via PSCAD simulation. For that purpose, the passive filters with the characteristics of Table 6.9 are placed onshore and offshore of the equivalent offshore wind farm, Figure 6.22.

These filters have the objective to reduce the harmonic levels at PCC, so, in order to compare the simulation results and deduce conclusions, in both cases (for offshore filters and onshore filters), the FFT of the current is performed at this point.

These simulation results are depicted in Table 6.10, in this table, three results are compared: results of the base scenario with onshore filters, results of the base scenario with offshore filters and results of the base scenario without filters. These results are for the case, when the transmission system is transmitting the nominal power, Figure 6.25.

	I_{350Hz}	I_{550Hz}	THD
Without filter	4	1.3	4.52
Onshore filter	1.96	1.15	2.43
Offshore filter	1.62	1.11	2.09

Table 6.10 Comparison of the amplitude of the harmonic currents in the PCC for different positions of the filters, while the wind farm is generating the nominal power.

Looking at Table 6.10 seems that the best location to place RLC filters is offshore, due to the fact that the THD at the PCC is smaller in comparison with the other options. Furthermore, with the passive filters placed offshore, it is possible to see a bigger reduction in all the selected individual harmonics. Besides, in offshore location there is the possibility to connect these filters to the medium voltage inter-turbine grid.

However, offshore location also has disadvantages, the access to the location is more difficult and the passive filters need a place to be located in the offshore platform.

Last of all, note that the passive filters definition carried out in the present analysis is based on the perfect knowledge of parameters, therefore, in real conditions where the parameters are not well known, passive solutions might not be suitable.

6.7 Chapter conclusions

The study presented in this chapter is focused on the evaluation of the frequency response of the offshore wind farm. This frequency response depends on design parameters such as: the cable length and characteristics, transformers connection and leakage inductance or inter-turbine grid's configuration. The analysis carried out estimates the potential risks on the voltage and current harmonic amplifications.

For that purpose, the state equations are a good approximation in order to estimate in an easy way the frequency response and main resonances of the system. The results obtained with this method are very similar to the simulation results in PSCAD.

As regards to the harmonic risk of the AC offshore wind farms, this kind of wind farms have the potential to amplify low order harmonics due to the iteration between the capacitive component of the submarine cable and the leakage inductance of the step-up transformer. From the results of this study, it is possible to observe, that the resonance frequency depends mainly on the characteristics of the submarine cable (its capacitive component).

The main resonance of the AC offshore wind farm from the viewpoint of the wind turbines is the same of the transmission systems resonance. The inter turbine grid, does not cause big variations in the frequency response and for different positions in the inter turbine grid, the frequency response is similar. However, the inter turbine grid causes "small resonances", which varies with the wind turbines position in the inter-turbine grid. This little resonance has less potential to amplify harmonic components, but, grid codes (like IEEE-519 standard) are more restrictive with the high order harmonics.

To avoid as far as possible the harmonic amplification in normal operation due to the resonance of the transmission system, one good option seems to choose a configuration which the resonance frequency of the transmission system coincides with one of the frequencies that the step up transformer does not allow to transmit, Figure 6.7.

Finally, highlight that the present analysis does not takes into account the effect of the control strategies of the wind turbines. These control strategies can be oriented to mitigate the resonance avoiding filters. In the same way, neither is taken into account further and more complex analysis about the harmonic risk or problems related to the iteration between the control strategies of the wind turbines.

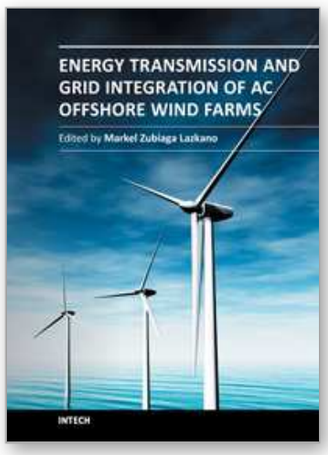

Energy Transmission and Grid Integration of AC Offshore Wind Farms

Edited by MSc Markel Zubiaga

ISBN 978-953-51-0368-4
Hard cover, 248 pages
Publisher InTech
Published online 21, March, 2012
Published in print edition March, 2012

This book analyses the key issues of the offshore wind farm's energy transmission and grid integration infrastructure. But, for this purpose, there are not evaluated all the electric configurations. In the present book is deeply evaluated a representative case. This representative case is built starting from three generic characteristics of an offshore wind farm: the rated power, the distance to shore and the average wind speed of the location. Thus, after a brief description of concepts related to wind power and several subsea cable modeling options, an offshore wind farm is modeled and its parameters defined to use as a base case. Upon this base case, several analyses of the key aspects of the connection infrastructure are performed. The first aspect to analyze is the management of the reactive power flowing through the submarine cable. Then, the undesired harmonic amplifications in the offshore wind farms due to the resonances and after this, transient over-voltage problems in the electric infrastructure are characterized. Finally, an offshore wind farm connection infrastructure is proposed in order to achieve the grid code requirements for a specific system operator, but not as a close solution, as a result of a methodology based on analyses and simulations to define the most suitable layout depending on the size and location of each offshore wind farm.

INTECH
open science | open minds

InTech Europe
University Campus STeP Ri
Slavka Krautzeka 83/A
51000 Rijeka, Croatia
Phone: +385 (51) 770 447
Fax: +385 (51) 686 166
www.intechopen.com

InTech China
Unit 405, Office Block, Hotel Equatorial Shanghai
No.65, Yan An Road (West), Shanghai, 200040, China
中国上海市延安西路65号上海国际贵都大饭店办公楼405单元
Phone: +86-21-62489820
Fax: +86-21-62489821

IntechOpen